Coordination of Semiquinone and Superoxide Radical Anions to the Zinc Ion in SOD Model Complexes that Act as the Key Step in Disproportionation of the Radical Anions

Hideki Ohtsu and Shunichi Fukuzumi*[a]

Abstract: Reactions of imidazolate-bridged Cu^{II}–Zn^{II} heterodinuclear and Cu^{II}–Cu^{II} homodinuclear complexes, $[Cu^{II}Zn^{II}(bdpi)(CH_3CN)_2](ClO_4)_3 \cdot 2CH_3CN$ (**1**) and $[Cu^{II}_2(bdpi)(CH_3CN)_2](ClO_4)_3 \cdot CH_3CN \cdot 3H_2O$ (**2**) (Hbdpi = 4,5-bis(di(2-pyridylmethyl)aminomethyl)imidazole), with the *p*-benzosemiquinone radical anion ($Q^{\bullet-}$) have been examined to provide mechanistic insight into the role of the Zn^{II} ion in copper–zinc superoxide dismutase (Cu,Zn-SOD). The addition of less than one equivalent of $Q^{\bullet-}$ to a deaerated solution of **1** or **2** in propionitrile at $-80\,^{\circ}C$ results in the oxidation of $Q^{\bullet-}$ accompanied by the appearance of a new absorption band at 585 nm due to the Cu^{I}–Q complex (**3** or **4**), the absorbance of which increases linearly with the increase in $Q^{\bullet-}$ concentration. Both the resonance Raman spectra of **3** and **4** exhibit a strong resonance-enhanced Raman band at 1580 cm^{-1}, which can be assigned to a CO stretching vibration in the Cu^{I}–Q complexes. Further addition of $Q^{\bullet-}$ to a deaerated solution of **3** in propionitrile results in the reduction of $Q^{\bullet-}$, whereas no reduction of $Q^{\bullet-}$ occurs with **4**, which does not contain the Zn^{II} ion. Thus, the coordination of $Q^{\bullet-}$ to the Zn^{II} ion is essential for the reduction of $Q^{\bullet-}$ by the Cu^{I} ion in **3**. The coordination of $O_2^{\bullet-}$ and $Q^{\bullet-}$ to the Zn^{II} ion has been confirmed by the electronic and ESR spectra of the $O_2^{\bullet-}$ and $Q^{\bullet-}$ complexes with mononuclear Zn^{II} complexes, $[Zn^{II}\{MeIm(Py)_2\}(CH_3CN)](ClO_4)_2$ (**5**) and $[Zn^{II}\{MeIm(Me)_2\}(H_2O)](ClO_4)_2$ (**6**) ($MeIm(Py)_2$ = (1-methyl-4-imidazolylmethyl)bis(2-pyridylmethyl)amine, $MeIm(Me)_2$ = (1-methyl-4-imidazolylmethyl)bis(6-methyl-2-pyridylmethyl)amine). The binding energies of $O_2^{\bullet-}$ with the Zn^{II} ion in **5** and **6** have been evaluated from the deviation of the $g_{\parallel}$ values of the ESR spectra from the free spin value.

Keywords: Cu,Zn-SOD · disproportionation · Lewis acids · *p*-benzosemiquinone · radical ions · superoxide ions

Introduction

Copper–zinc superoxide dismutase (Cu,Zn-SOD) contains an imidazolate-bridged Cu^{II}–Zn^{II} heterodinuclear metal center in its active site.[1–9] The copper ion is coordinated to the four imidazole N atoms of histidine residues and a solvent (H_2O) in a distorted square-pyramidal geometry, while the zinc ion, located at a distance of 6.2 Å from the copper ion, is coordinated to a carboxylato O atom of an aspartic acid residue and three imidazole N atoms of histidine residues in a distorted tetrahedral structure.[1, 2] This enzyme protects cells against oxidative damage by catalyzing the disproportionation (dismutation) of the toxic superoxide ion ($O_2^{\bullet-}$) to dioxygen (O_2) and hydrogen peroxide (H_2O_2).[1] Under physiological conditions, the disproportionation of $O_2^{\bullet-}$ must proceed very rapidly, that is at the diffusion-limited rate, in order to prevent the uncontrolled oxidation of cells by $O_2^{\bullet-}$ and/or its conjugated acid $HO_2^{\bullet}$.[1] The Cu^{II} form of the enzyme is reduced by $O_2^{\bullet-}$ to produce O_2 and the reduced Cu^{I} enzyme which is oxidized by another $O_2^{\bullet-}$ molecule to yield H_2O_2.[1–13] In this case both the oxidation and reduction of $O_2^{\bullet-}$ should be accelerated by Cu,Zn-SOD. We have previously reported that an important role of the Zn^{II} ion in the imidazolate-bridged Cu^{II}–Zn^{II} complex is to accelerate an outer-sphere electron transfer from $O_2^{\bullet-}$ to produce the Cu^{I}–Zn^{II} complex when the free energy change of electron transfer becomes thermodynamically more favorable as compared to that without Zn^{II} ion.[14] The presence of the Zn^{II} ion, which can act as a Lewis acid may also accelerate an electron transfer from the Cu^{I}–Zn^{II} complex to $O_2^{\bullet-}$, since $O_2^{\bullet-}$ can form a complex with metal ions acting as a Lewis acid to accelerate the electron-transfer reduction of $O_2^{\bullet-}$.[15] Such an acceleration for the reduction of $O_2^{\bullet-}$ can also be attained by a Brønsted acid instead of a Lewis acid since Valentine et al. reported that the reduction of $O_2^{\bullet-}$ by the zinc-deficient SOD form is acid catalyzed.[13] Thus, the essential part of the catalysis of Cu,Zn-SOD is the acceleration of the reduction of

[a] Prof. S. Fukuzumi, H. Ohtsu
Department of Material and Life Science
Graduate School of Engineering, Osaka University
CREST, JAPAN Science and Technology Corporation
2-1 Yamada-oka, Suita, Osaka 565-0871 (Japan)
Fax: (+81) 6-6879-7370
E-mail: fukuzumi@chem.eng.osaka-u.ac.jp

  0947-6539/01/0722-4947 $ 17.50+.50/0

$O_2^{\bullet-}$ by the Cu^I center. It has been one of the central issues in bioinorganic chemistry to clarify how the Zn^{II} ion can facilitate the reduction of $O_2^{\bullet-}$ in Cu,Zn-SOD.[1–13] However, the instability of reaction intermediates and the lack of appropriate model complexes that contain the substrate-binding sites has so far precluded the study of the essential role of the Zn^{II} ion in the catalytic function of Cu,Zn-SOD.[16–21]

We recently prepared the first imidazolate-bridged Cu^{II}–Zn^{II} heterodinuclear complex, $[Cu^{II}Zn^{II}(bdpi)(CH_3CN)_2](ClO_4)_3\cdot 2CH_3CN$ (**1**) with a newly designed dinucleating ligand, Hbdpi (Hbdpi = 4,5-bis(di(2-pyridylmethyl)aminomethyl)imidazole).[14] The Cu^{II}–Cu^{II} homodinuclear complex, $[Cu^{II}_2(bdpi)(CH_3CN)_2](ClO_4)_3\cdot CH_3CN\cdot 3H_2O$ (**2**), was also prepared in order to compare its properties with the heterodinuclear Cu^{II}–Zn^{II} complex.[4] In these SOD model complexes each metal ion is pentacoordinated with one position taken by a solvent molecule, which can be readily replaced by a substrate.

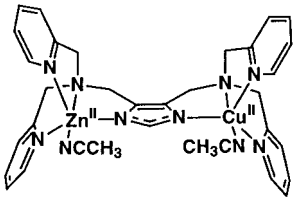

$[Cu^{II}Zn^{II}(bdpi)(CH_3CN)_2]^{3+}$ (1)

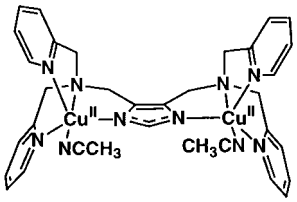

$[Cu^{II}_2(bdpi)(CH_3CN)_2]^{3+}$ (2)

This study reports an essential role of the Zn^{II} ion observed as a drastic difference in the stoichiometric disproportionation of the *p*-benzosemiquinone radical anion ($Q^{\bullet-}$) with the imidazolate-bridged Cu^{II}–Zn^{II} heterodinuclear (**1**) and Cu^{II}–Cu^{II} homodinuclear (**2**) complexes in propionitrile (EtCN). The coordination of $Q^{\bullet-}$ to the Zn^{II} ion in **1** is shown to be indispensable for the reduction of $Q^{\bullet-}$ by the Cu^I ion produced by the electron transfer from $Q^{\bullet-}$ to the Cu^{II} ion in **1**. We also report herein the detection of $Zn^{II}-O_2^{\bullet-}$ complexes by using the mononuclear Zn^{II} complexes of $[Zn^{II}\{MeIm(Py)_2\}(CH_3CN)](ClO_4)_2$ (**5**) and $[Zn^{II}\{MeIm(Me)_2\}(H_2O)](ClO_4)_2$ (**6**) ($MeIm(Py)_2$ = (1-methyl-4-imidazolylmethyl)-bis(2-pyridylmethyl)amine, $MeIm(Me)_2$ = (1-methyl-4-imidazolylmethyl)bis(6-methyl-2-pyridylmethyl)amine). The binding energies of $O_2^{\bullet-}$ with the Zn^{II} ion in **5** and **6** can be evaluated from deviation of the $g_{\|}$ values from the free spin value by the ESR measurements.[15]

Results and Discussion

Oxidation of the *p*-benzosemiquinone radical anion by imidazolate-bridged Cu^{II}–Zn^{II} heterodinuclear and Cu^{II}–Cu^{II} homodinuclear complexes: The addition of less than one equivalent of $Q^{\bullet-}$ to a deaerated solution of $[Cu^{II}Zn^{II}(bdpi)(CH_3CN)_2](ClO_4)_3\cdot 2CH_3CN$ (**1**) in EtCN resulted in the appearance of a new absorption band at 585 nm, the absorbance of which increased linearly with an increase in the $Q^{\bullet-}$ concentration, as shown in Figure 1a. The appearance

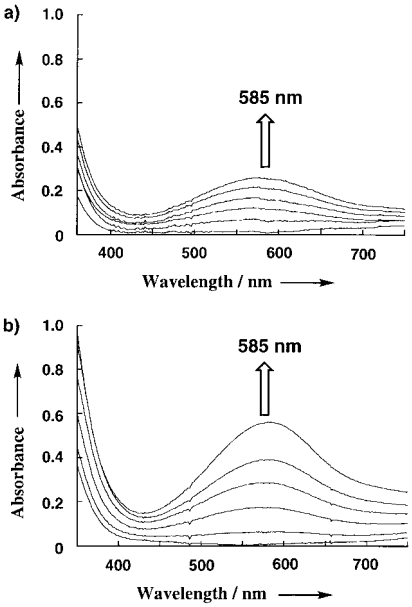

Figure 1. Absorption spectral changes of the titration observed upon addition of $Q^{\bullet-}$: a) 0, 0.2, 0.4, 0.6, 0.8, 1.0 equiv for $[Cu^{II}Zn^{II}(bdpi)(CH_3CN)_2]^{3+}$ (**1**); b) 0, 0.4, 0.8, 1.2, 1.6, 2.0 equiv for $[Cu^{II}_2(bdpi)(CH_3CN)_2]^{3+}$ (**2**) into a solution of **1** in EtCN (1.0×10^{-4} M) and **2** (1.0×10^{-4} M) at 193 K.

of the same absorption band ($\lambda_{max}=585$ nm) is observed when **1** is replaced by $[Cu^{II}_2(bdpi)(CH_3CN)_2](ClO_4)_3\cdot CH_3CN\cdot 3H_2O$ (**2**) for the reaction with $Q^{\bullet-}$. In the case of **2**, however, the absorbance at 585 nm increases linearly with an increase in the $Q^{\bullet-}$ concentration up to two equivalents of $Q^{\bullet-}$ (Figure 1b).

Since the one-electron oxidation potential (E^0_{ox} *vs* SCE) of $Q^{\bullet-}$ (-0.51 V), which is equal to the one-electron reduction potential of Q,[22] is more negative than the one-electron reduction potential (E^0_{red} *vs* SCE) of the Cu^{II} center of **1** (-0.03 V),[14] an electron transfer from $Q^{\bullet-}$ to the Cu^{II} center should occur, as shown in Scheme 1, to yield the Cu^I–Q complex (**3**), which may have the metal-to-ligand change transfer (MLCT) band at 585 nm. In the case of **2**, two equivalents of $Q^{\bullet-}$ may be oxidized (Scheme 1), since the E^0_{ox} value of $Q^{\bullet-}$ is still more negative than the second one-electron reduction potential of **2** for the other Cu^{II} center (-0.31 V).[14] This may be the reason why two equivalents of $Q^{\bullet-}$ can be oxidized by **2** to give the 2:1 complex between Q and the Cu^I center (**4**), which has the same absorption band at 585 nm, and the absorbance is twice as large as that of **3**. The Cu^I–Q complexes **3** and **4** should be diamagnetic, and it was confirmed that the reaction mixtures of one and two equivalents of $Q^{\bullet-}$ with **1** and **2**, respectively, were ESR silent at 77 K.

The resonance Raman spectra of intermediates **3** and **4** in an acetonitrile (CH_3CN) solution at 298 K (laser excitation wavelength: 632.8 nm) are shown in Figure 2a and b, respectively, which reveal the same strong resonance-enhanced Raman bands at 1580 cm^{-1}. The resonance Raman frequency is significantly higher than that reported for the CO stretching vibration of free $Q^{\bullet-}$ (1435 cm^{-1}), in which the CO bond order is estimated from the Raman data to be 1.5,[23] but lower than

0947-6539/01/0722-4948 $ 17.50+.50/0 *Chem. Eur. J.* **2001**, *7*, No. 22

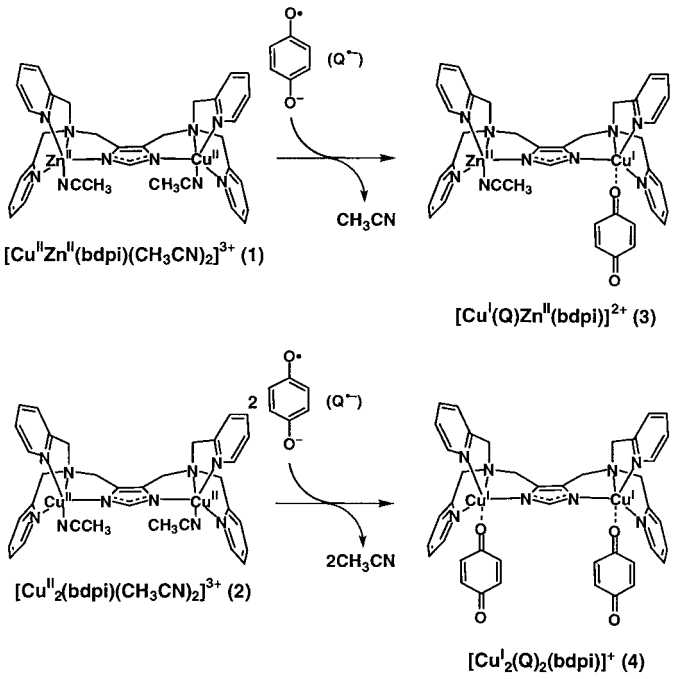

Scheme 1. Electron transfer reactions of **1** and **2** to give complexes **3** and **4**, respectively. Counter ions and solvent of crystallization omitted for clarity.

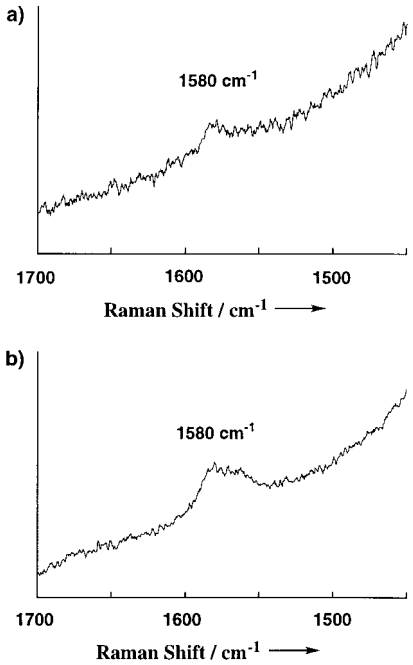

Figure 2. Resonance Raman spectra obtained with 632.8 nm excitation upon a) one and b) two equivalents of $Q^{\bullet-}$ in a solution of complexes **1** and **2** in CH_3CN at 298 K, respectively.

that of neutral *p*-benzoquinone (1651 cm^{-1}).[24, 25] Thus, the resonance Raman bands of **3** and **4** at 1580 cm^{-1} can be assigned with reasonable certainty to a CO stretching vibration in the Cu^{I}–Q complexes $[Cu^{I}(Q)Zn^{II}(bdpi)]^{2+}$ and $[Cu^{I}_2(Q)_2(bdpi)]^{+}$, respectively.

Reduction of semiquinone radical anion by a SOD model complex: The addition of two equivalents of $Q^{\bullet-}$ to an intermediate **3** results in no further increase in the absorption band at 585 nm, but the decay of the absorption band due to $Q^{\bullet-}$ ($\lambda_{max} = 422$ nm) is observed (Figure 3a). The rate of decay obeys first-order kinetics (see the inset of Figure 3a), and the rate constant (k_{obs}) at 193 K is determined to be 4.0×10^{-1} s^{-1}. Since the binding of $Q^{\bullet-}$ to the Mg^{II} ion is known to facilitate

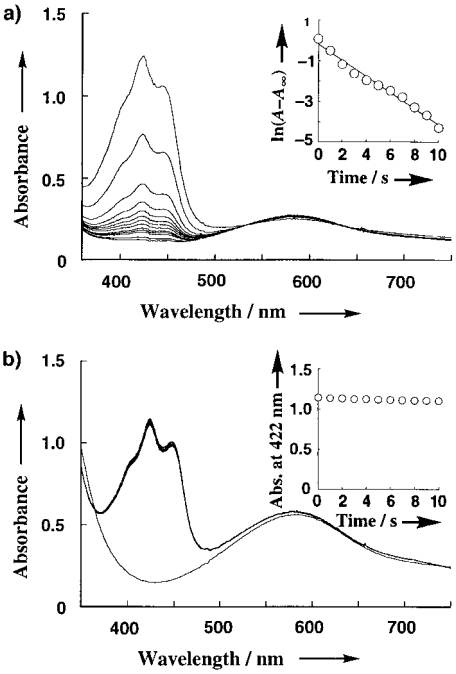

Figure 3. Spectral changes observed upon the addition of two equivalents of $Q^{\bullet-}$ into the solution of a) **3** and b) **4** in EtCN at 193 K; taken at 1 s intervals. Insets: a) first-order plot of the absorption change for **3** and b) time course of the absorption change for **4** at 422 nm.

the electron-transfer reduction of $Q^{\bullet-}$,[26] the complexation of $Q^{\bullet-}$ with the Zn^{II} ion in $[Cu^{I}(Q)Zn^{II}(bdpi)]^{2+}$ may also facilitate an intramolecular electron transfer from the Cu^{I} center to $Q^{\bullet-}$ bound to the Zn^{II} center as shown in Scheme 2. The disappearance of $Q^{\bullet-}$ was also confirmed by ESR measurement.

When three or four equivalents of $Q^{\bullet-}$ are added to an intermediate **3**, however, one or two equivalents of $Q^{\bullet-}$ remain unreacted judging from the absorbance at 422 nm ($\varepsilon = 6000\,M^{-1}cm^{-1}$). Thus, the stoichiometry of $Q^{\bullet-}$ to an intermediate **3** has been determined to be 2:1. This result indicates that one of the $Q^{\bullet-}$ that binds to the Zn^{II} ion is reduced by the Cu^{I} ion and the other coordinates to the Cu^{II} ion, which is oxidized by $Q^{\bullet-}$ bound to the Zn^{II} ion (Scheme 2).

The formation of $[Cu^{I}(Q)Zn^{II}(Q^{2-})(bdpi)]$ is confirmed by the ESI mass spectrum, as shown in Figure 4, in which the protonated form, $[Cu^{I}(Q)Zn^{II}(QH^{-})(bdpi)]^{+}$ ($m/z = 727$) is observed. The natural-isotope abundance pattern agrees well with the simulated one as shown in Figure 4.

Although observation of the ESI mass spectrum of $[Cu^{I}(Q)Zn^{II}(QH^{-})(bdpi)]^{+}$ by itself does not confirm the stoichiometry in Scheme 2, the spectral change in Figure 3 and the disappearance of the ESR signal of $Q^{\bullet-}$ taken together demonstrate the validity of this stoichiometry.

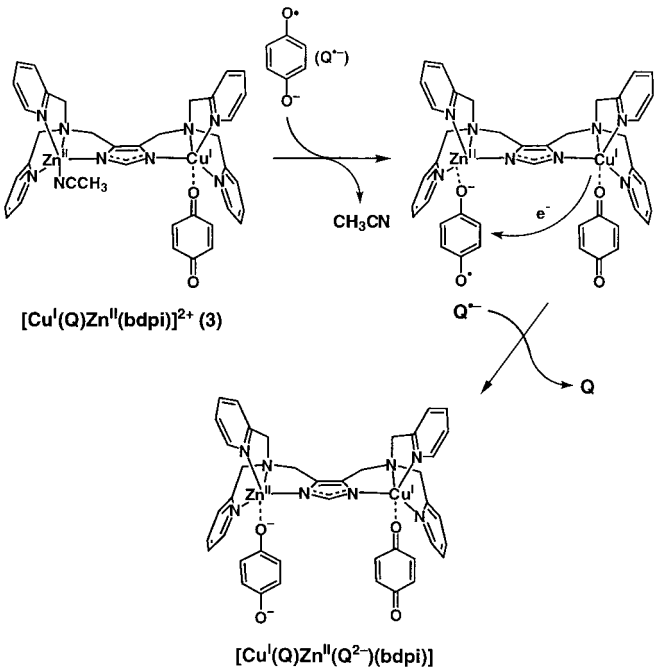

Scheme 2. Electron transfer reaction of **3** and subsequent intramolecular electron transfer. Counter ions and solvent of crystallization omitted for clarity.

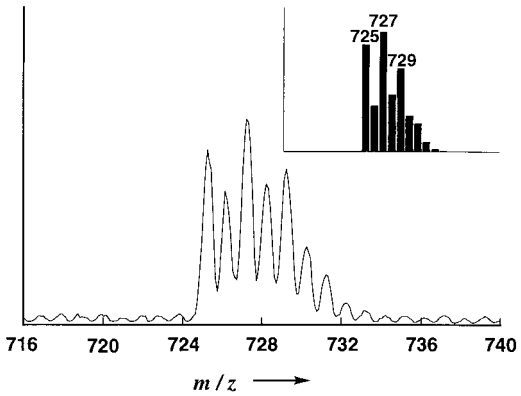

Figure 4. ESI mass spectrum of $[Cu^{I}(Q)Zn^{II}(QH^{-})(bdpi)]^{+}$ in CH_3CN at 298 K. Inset: calculated natural isotope abundance pattern of $[Cu^{I}(Q)Zn^{II}(QH^{-})(bdpi)]^{+}$.

In sharp contrast to the case of the Cu^{II}–Zn^{II} heterodinuclear complex (**1**), the addition of more than two equivalents of $Q^{\bullet-}$ to the Cu^{II}–Cu^{II} homodinuclear complex (**2**) results in the appearance of an absorption band due to $Q^{\bullet-}$, which is stable, and no reduction of $Q^{\bullet-}$ occurs (Figure 3b). In the case of **2**, there is no Zn^{II} center available to facilitate the reduction of $Q^{\bullet-}$ and therefore no reduction of $Q^{\bullet-}$ occurs. Thus, the coordination of $Q^{\bullet-}$ to the Zn^{II} ion in **3** derived from **1** is indispensable for the reduction of $Q^{\bullet-}$ by the Cu^{I} center of **3** in EtCN (Scheme 2).

Since $Q^{\bullet-}$ coordinated to the Zn^{II} ion in **3** undergoes a facile electron-transfer reaction with the Cu^{I} center of **3**, the coordination of $Q^{\bullet-}$ to the Zn^{II} ion has been confirmed by the spectroscopic detection of the Zn^{II}–$Q^{\bullet-}$ complex by using a mononuclear Zn^{II} complex $[Zn^{II}\{MeIm(Py)_2\}(CH_3CN)](ClO_4)_2$ (**5**) ($MeIm(Py)_2$ = (1-methyl-4-imidazolylmethyl)-bis(2-pyridylmethyl)amine) as shown in Scheme 3. The addition of a large excess of complex **5** to a solution of $Q^{\bullet-}$ in EtCN at 193 K resulted in the appearance of a new absorption band at 570 nm, which disappeared at higher temperatures as shown in Figure 5.

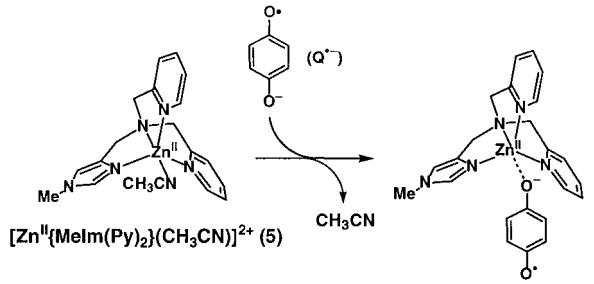

Scheme 3. Electron transfer reaction of the mononuclear **5**. Counter ions and solvent of crystallization omitted for clarity.

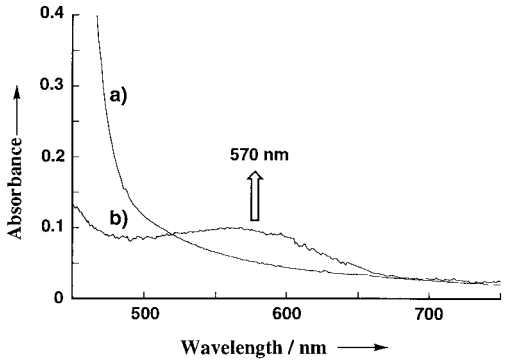

Figure 5. UV/Vis Spectra of a) $Q^{\bullet-}$ (2.5×10^{-4} M) and b) the Zn^{II}–$Q^{\bullet-}$ complex observed upon addition of a large excess of $[Zn^{II}\{MeIm(Py)_2\}(CH_3CN)]^{2+}$ (**5**) to a solution of $Q^{\bullet-}$ in EtCN at 193 K.

We have previously reported that the Mg^{II}–$Q^{\bullet-}$ complex has an characteristic absorption band at 590 nm due to a red-shifted $\pi-\pi^*$ transition of the $Q^{\bullet-}$ complex.[26, 27] The absorption band at 570 nm of the Zn^{II}–$Q^{\bullet-}$ complex, which is slightly blue-shifted compared with the Mg^{II}–$Q^{\bullet-}$ complex, can also be assigned to a $\pi-\pi^*$ transition of $[Zn^{II}(Q^{\bullet-})\{MeIm(Py)_2\}]^{+}$. One of the disproportionation products was confirmed by the ESI mass spectrum, which exhibited a signal at $m/z = 466$, as shown in Figure 6. The

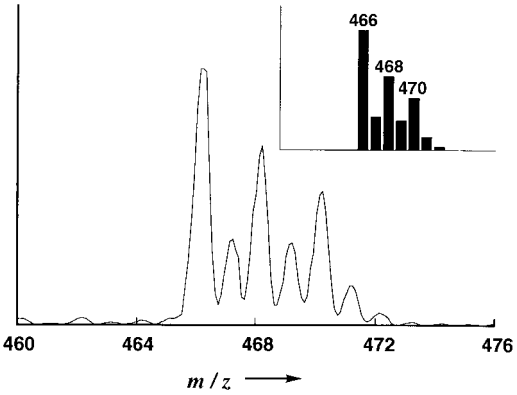

Figure 6. ESI mass spectrum of $[Zn^{II}(QH^{-})\{MeIm(Py)_2\}]^{+}$ in CH_3CN at 298 K. Inset: calculated natural isotope abundance pattern of $[Zn^{II}(QH^{-})\{MeIm(Py)_2\}]^{+}$.

0947-6539/01/0722-4950 $ 17.50+.50/0 *Chem. Eur. J.* **2001**, *7*, No. 22

observed mass and isotope patterns agree with the ion $[Zn^{II}(QH^{-})\{MeIm(Py)_2\}]^{+}$, which is the protonated form of $[Zn^{II}(Q^{2-})\{MeIm(Py)_2\}]$.

Zn^{II}-superoxide complexes with mononucleating ligands: The superoxide ion is produced by the photoinduced reduction of O_2 by dimeric 1-benzyl-1,4-dihydronicotinamide $[(BNA)_2]$ in EtCN,[28] which can act as a unique two-electron donor[29] as shown in [Eq. (1)].

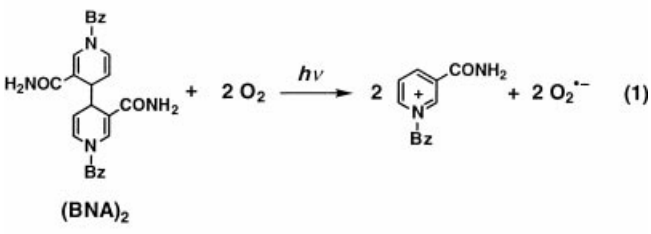

When an oxygen-saturated EtCN solution containing $(BNA)_2$ was irradiated with a high-pressure mercury lamp, photochemically formed $O_2^{\bullet-}$ was detected by the ESR spectrum in frozen EtCN at 133 K. The ESR spectrum shows a typical anisotropic signal with $g_{\parallel} = 2.0900$ and $g_{\perp} = 2.0050$.[30]

The addition of Zn^{II} complexes, $[Zn^{II}\{MeIm(Py)_2\}(CH_3CN)](ClO_4)_2$ (**5**) and $[Zn^{II}\{MeIm(Me)_2\}(H_2O)](ClO_4)_2$ (**6**), ($MeIm(Me)_2$ = (1-methyl-4-imidazolylmethyl)-bis(6-methyl-2-pyridylmethyl)amine) to a solution of $O_2^{\bullet-}$ in EtCN results in formation of the $O_2^{\bullet-}$ complexes (see Scheme 4 for the case of **5**). The ESR spectra of the Zn^{II}–$O_2^{\bullet-}$

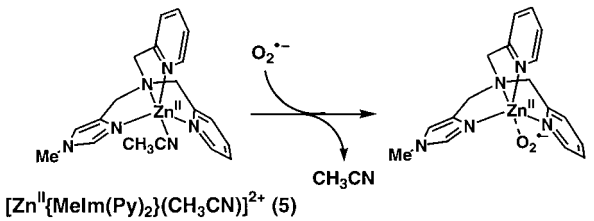

Scheme 4. Formation of an O_2 complex with **5**. Counter ions and solvent of crystallization omitted for clarity.

complexes measured at 133 K are shown in Figure 7. The $g_{\parallel}$ values of these Zn^{II}–$O_2^{\bullet-}$ complexes are significantly smaller than the value of free $O_2^{\bullet-}$ due to the complexation of the Zn^{II} ion with $O_2^{\bullet-}$.[31]

The $g_{\parallel}$ value gives valuable information concerning the binding strength of $O_2^{\bullet-}$ and metal ions.[15] The deviation of the $g_{\parallel}$ value from the free spin value ($g_e = 2.0023$) is caused by the spin–orbit interaction as given by Equation (2),[32]

$$g_{\parallel} = g_e + 2\sqrt{\frac{\lambda^2}{\lambda^2 + \Delta E^2}} \qquad (2)$$

in which λ is the spin–orbit coupling constant of oxygen, which is known to be 0.0140 eV,[33, 34] and ΔE is the energy splitting of π_g levels due to complex formation between $O_2^{\bullet-}$ and the Zn^{II} ion. Under the conditions that $\Delta E \gg \lambda$, [Eq. (2)] is reduced to a simple relation, $g_{\parallel} = g_e + 2\lambda/\Delta E$. Thus, the $g_{\parallel}$ values are used to determine the ΔE values, since they are the most sensitive to the ΔE values.[15] The ΔE values of the Zn^{II}–$O_2^{\bullet-}$ complexes have been evaluated from deviation of the $g_{\parallel}$ values from the free-spin value and are listed in Table 1 with the $g_{\parallel}$ values. The ΔE values of the $O_2^{\bullet-}$ complex with **6**

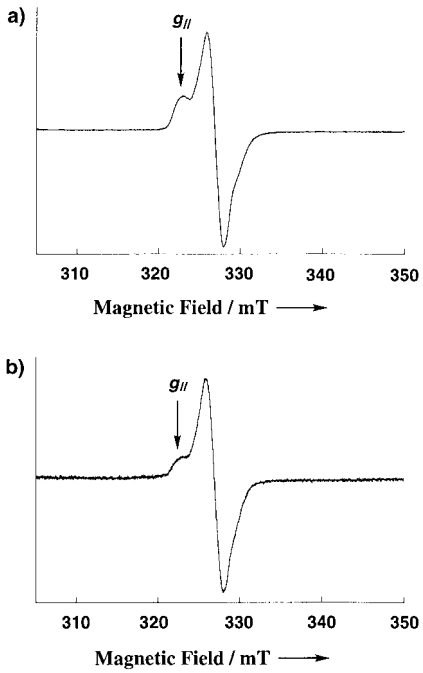

Figure 7. ESR spectra of a) $[Zn^{II}(O_2^{\bullet-})\{MeIm(Py)_2\}]^{+}$ and b) $[Zn^{II}(O_2^{\bullet-})\{MeIm(Me)_2\}]^{+}$ in frozen EtCN at 133 K.

Table 1. The $g_{\parallel}$ values and ΔE values of ESR spectra of Zn^{II}-$O_2^{\bullet-}$ complexes

Complex	$g_{\parallel}$	ΔE [eV]
$O_2^{\bullet-}$	2.0900	0.319
$[Zn^{II}(O_2^{\bullet-})\{MeIm(Py)_2\}]^{2+}$	2.0351	0.854
$[Zn^{II}(O_2^{\bullet-})\{MeIm(Me)_2\}]^{2+}$	2.0344	0.872

(0.872 eV) and **5** (0.854 eV) are significantly larger than those of $O_2^{\bullet-}$ complexes with other divalent metal ions (Mg^{II} ion: 0.65 eV, Ca^{II} ion: 0.58 eV, Sr^{II} ion: 0.52 eV, and Ba^{II} ion: 0.49 eV);[15] this reflects the strong Lewis acidity of the Zn^{II} ion relative to other divalent metal ions.[35] The larger ΔE value of the $O_2^{\bullet-}$ complex with **6** (0.872 eV) than with **5** (0.854 eV) may be ascribed to the increased Lewis acidity of the Zn^{II} ion in **6** due to the steric effect of the *o*-methyl group of the pyridine moiety of **6**.

Further evidence of the steric effect of the *o*-methyl group in **6** comes from ^{19}F NMR experiments on the fluoride ion complexes. The addition of one equivalent of Bu_4NF to a solution of **5** or **6** in CD_3CN in the presence of an internal standard, trifluorotoluene (0 ppm), exhibited new signals at $\delta = -157$ and -108, respectively. The ^{19}F NMR signal of the F^{-} complex with **6** at lower magnetic field than that with **5** indicates that the Lewis acidity of the Zn^{II} ion in **6** is stronger than in **5**. This is consistent with the larger ΔE value of the $O_2^{\bullet-}$ complex with **6** as compared with **5**.

Conclusion

The Zn^{II} ion in the imidazolate-bridged Cu^{II}–Zn^{II} heterodinuclear complex **1** has been shown to be indispensable for the reduction of $Q^{\bullet-}$ by the Cu^{I} center, which is formed by the oxidation of $Q^{\bullet-}$ by the Cu^{II} center of **1**, through coordination of $Q^{\bullet-}$ to the Zn^{II} ion (Scheme 2), since no reduction of $Q^{\bullet-}$ by the Cu^{I} center occurs in the corresponding Cu^{II}–Cu^{II} homodinuclear complex **2** in EtCN. The binding energies of the Zn^{II}–$O_2^{\bullet-}$ complexes, which reflect the Lewis acidity of the Zn^{II} ion, have been evaluated from the deviation of the $g_{\|}$ values of ESR spectra from the free-spin value.

Experimental Section

Materials: All chemicals used for the ligand synthesis were commercial products of the highest available purity and were further purified by the standard methods.[36] All solvents were also purified by standard methods before use.[36] The dimeric 1-benzyl-1,4-dihydronicotinamide [$(BNA)_2$] was prepared according to the literature.[37] *p*-Benzoquinone and hydroquinone were purchased from the Tokyo Chemical Industry Co., Ltd., and recrystallized from ethanol prior to use. Tetra-*n*-butylammonium hydroxide was purchased from Aldrich and used as received. The solution of the *p*-benzosemiquinone radical anion ($Q^{\bullet-}$) was prepared in comproportionation between *p*-benzoquinone and hydroquinone in the presence of tetra-*n*-butylammonium hydroxide as described in the literature.[38]

Synthesis of ligands: All ligands used in this study were prepared according to the following procedures and the structures of the products were confirmed by the analytical data (vide infra).

4,5-Bis[di(2-pyridylmethyl)aminomethyl]imidazole (Hbdpi), (1-methyl-4-imidazolylmethyl)bis(2-pyridylmethyl)amine [MeIm(Py)$_2$]: This compound was prepared as described previously.[14]

(1-Methyl-4-imidazolylmethyl)bis(6-methyl-2-pyridylmethyl)amine [MeIm(Me)$_2$]: The same procedure as that for the synthesis of MeIm(Py)$_2$[14] was employed to obtain MeIm(Me)$_2$ by using bis(6-methyl-2-pyridylmethyl)amine instead of bis(2-pyridylmethyl)amine. Yield: 2.50 g (97.3%); ^{1}H NMR (400 MHz, $CDCl_3$, 25 °C, TMS) $\delta = 2.51$ (s, 6H; CH_3Py), 3.62 (s, 3H; CH_3Im), 3.69 (s, 2H; NCH_2Im), 3.83 (s, 4H; NCH_2Py), 6.87 (s, 1H; Im), 6.97 (d, $J = 5.2$ Hz, 2H; Py), 7.36 (s, 1H; Im), 7.48 (d, $J = 5.2$ Hz, 2H; Py), 7.53 (t, $J = 5.2$ Hz, 2H; Py). ^{13}C NMR (100 MHz, $CDCl_3$, 25 °C, TMS) $\delta = 24.1$ (CH_3Py), 33.0 (CH_3Im), 51.3 (CH_2), 59.5 (CH_2), 118.5 (Im), 119.4 (Py), 120.9 (Py), 136.3 (Py), 137.0 (Im), 139.3 (Im), 157.0 (Py), 159.1 (Py).

Synthesis of Complexes: All complexes used in this study were prepared according to the following procedures and the products were confirmed by the analytical data (vide infra).

[Cu^{II}Zn^{II}(bdpi)(CH$_3$CN)$_2$](ClO$_4$)$_3$·2CH$_3$CN (1), [Cu$^{II}_2$(bdpi)(CH$_3$CN)$_2$](ClO$_4$)$_3$·CH$_3$CN·3H$_2$O (2): These complexes were prepared as described previously.[14]

[Zn^{II}(MeIm(Py)$_2$)(CH$_3$CN)](ClO$_4$)$_2$ (5): $Zn(ClO_4)_2 \cdot 6H_2O$ (0.37 g, 1.0×10^{-3} M) in methanol (10 mL) was added dropwise to a solution of MeIm(Py)$_2$ (0.29 g, 1.0×10^{-3} M) in methanol (10 mL). After the mixture had stood for a few days at room temperature, the microcrystals that had precipitated were isolated and recrystallized from CH_3CN. Yield: 0.365 g (60%); ESI MS data: m/z: 456 $[M - ClO_4]^+$; elemental analysis calcd (%) for $C_{19}H_{23}N_6Zn_1Cl_2O_{8.5}$: C 37.55, H 3.81, N 13.83; found: C 37.43, H 3.49, N 13.95.

[Zn^{II}(MeIm(Me)$_2$)(H$_2$O)](ClO$_4$)$_2$ (6): was prepared in the same manner as **5** but by using the MeIm(Me)$_2$ ligand instead of MeIm(Py)$_2$. Yield: 0.396 g (64%); ESI MS data: m/z: 484 $[M - ClO_4]^+$; elemental analysis calcd (%) for $C_{19}H_{27}N_5Zn_1Cl_2O_{10}$: C 36.70, H 4.38, N 11.26; found: C 36.43, H 3.81, N 11.25.

Spectral measurements: Electronic spectra were measured with a Hewlett–Packard HP8452A or 8453 diode-array spectrophotometer with a Unisoku thermostated cell holder designed for low-temperature experiments (fixed within ±0.5 °C). After the deaerated solution of the SOD model complex (1.0×10^{-4} M) in the cell had been kept at the desired temperature for several minutes, semiquinone radical anion was added with a syringe. Formation of the intermediates was monitored by the absorption change at 585 nm. The rate constant for the stoichiometric disproportionation of $Q^{\bullet-}$ (k_{obs}) was determined by monitoring the decrease in the absorption band due to $Q^{\bullet-}$ ($\lambda_{max} = 422$ nm).

^{1}H, ^{13}C, and ^{19}F NMR measurements were performed with a JEOL JNM-GSX-400 (400 MHz) NMR spectrometer.

ESR spectra were taken on a JEOL JES-RE1X X-band spectrometer equipped with an attached variable temperature apparatus under non-saturating microwave power conditions. A quartz ESR tube (4.5 mm i.d.) containing an oxygen-saturated solution of $(BNA)_2$ (1.0×10^{-4} M) in EtCN and a Zn^{II} complex (5.0×10^{-3} M) was irradiated in the cavity of the ESR spectrometer with the light of a 1000 W high-pressure Hg lamp focused through an aqueous filter. All the spectra were recorded at 133 K. The *g* values were calibrated with a Mn^{II} marker used as a reference.

Resonance Raman spectra were excited at 632.8 nm with a He-Ne laser and detected with a JASCO NR-1800 triple polychromator equipped with a liquid-nitrogen-cooled Princeton Instruments CCD detector. Raman measurements were carried out with a spinning cell and the laser power was adjusted to 50 mW at the sample point. Raman shifts were calibrated by using acetonitrile, with the accuracy of the peak positions of the Raman bands being ±1 cm^{-1}.

ESI mass spectra were obtained with an API150 triple-quadrupole mass spectrometer (PE-Sciex) in positive-ion detection mode, equipped with an ion spray interface. The sprayer was held at a potential of 5.0 kV, and compressed N_2 was employed to assist liquid nebulization. The positive-ion ESI mass spectra were measured in the range m/z 100–1000.

Acknowledgements

We are grateful to Mituo Ohama, Graduate School of Science, Osaka University, for the measurements of resonance Raman spectra. This work was partially supported by a Grant-in-Aid for Scientific Research Priority Area (No. 11228205) from the Ministry of Education, Science, Sports and Culture, Japan.

[1] a) J. M. McCord, I. Fridovich, *J. Biol. Chem.* **1969**, *244*, 6049–6055; b) I. Fridovich, *J. Biol. Chem.* **1989**, *264*, 7761–7764; c) I. Fridovich, *Annu. Rev. Biochem.* **1995**, *64*, 97–112.
[2] J. A. Tainer, E. D. Getzoff, J. S. Richardson, D. C. Richardson, *Nature* **1983**, *306*, 284–287.
[3] I. Bertini, L. Banci, M. Piccioli, *Coord. Chem. Rev.* **1990**, *100*, 67–103.
[4] I. Bertini, S. Mangani, M. S. Viezzoli, *Adv. Inorg. Chem.* **1998**, *45*, 127–250.
[5] J. A. Tainer, E. D. Getzoff, K. M. Beem, J. S. Richardson, D. C. Richardson, *J. Mol. Biol.* **1982**, *160*, 181–217.
[6] E. M. Fielden, P. B. Roberts, R. C. Bray, D. J. Lowe, G. N. Mautner, G. Rotilio, L. Calabrese, *Biochem. J.* **1974**, *139*, 49–60.
[7] L. M. Ellerby, D. E. Cabelli, J. A. Graden, J. S. Valentine, *J. Am. Chem. Soc.* **1996**, *118*, 6556–6561.
[8] T. J. Lyons, E. B. Gralla, J. S. Valentine, *Met. Ions Biol. Syst.* **1999**, *36*, 125–177.
[9] A. L. Lamb, A. K. Wernimont, R. A. Pufahl, T. V. O'Halloran, A. C. Rosenzweig, *Nat. Struct. Biol.* **1999**, *6*, 724–729.
[10] K. Dijinovic, F. Polticelli, A. Desideri, G. Rotilio, K. S. Wilson, M. Bolognesi, *J. Mol. Biol.* **1994**, *240*, 179–183.
[11] G. Rotilio, R. C. Bray, E. M. Fielden, *Biochim. Biophys. Acta* **1972**, *268*, 605–609.
[12] D. Klug-Roth, I. Fridovich, J. Rabani, *J. Am. Chem. Soc.* **1973**, *95*, 2786–2790.
[13] P. J. Hart, M. M. Balbirnie, N. L. Ogihara, A. M. Nersissian, M. S. Weiss, J. S. Valentine, D. A. Eisenberg, *Biochemistry* **1999**, *38*, 2167–2178.
[14] H. Ohtsu, Y. Shimazaki, A. Odani, O. Yamauchi, S. Itoh, S. Fukuzumi, *J. Am. Chem. Soc.* **2000**, *122*, 5733–5741.
[15] S. Fukuzumi, K. Ohkubo, *Chem. Eur. J.* **2000**, *6*, 4532–4535.

  0947-6539/01/0722-4952 $ 17.50+.50/0

[16] M. Sato, S. Nagae, M. Uehara, J. Nakaya, *J. Chem. Soc. Chem. Commun.* **1984**, 1661–1663.
[17] Q. Lu, Q. H. Luo, A. B. Dai, Z. Y. Zhou, G. Z. Hu, *J. Chem. Soc. Chem. Commun.* **1990**, 1429–1431.
[18] M. Zongwan, C. Dong, T. Wenxia, Y. Kaibei, L. Li, *Polyhedron* **1992**, *11*, 191–196.
[19] J.-L. Pierre, P. Chautemps, S. Refaif, C. Beguin, A. E. Marzouki, G. Serratrice, E. Saint-Aman, P. Rey, *J. Am. Chem. Soc.* **1995**, *117*, 1965–1973.
[20] J.-L. Pierre. *Chem. Soc. Rev.* **2000**, *29*, 251–257.
[21] Z.-W. Mao, M.-Q. Chen, X.-S. Tan, J. Liu, W.-X. Tang, *Inorg. Chem.* **1995**, *34*, 2889–2893.
[22] S. Fukuzumi, S. Koumitsu, K. Hironaka, T. Tanaka, *J. Am. Chem. Soc.* **1987**, *109*, 305–316.
[23] R. H. Schuler, G. N. R. Tripathi, M. F. Prebenda, D. M. Chaipman, *J. Phys. Chem.* **1983**, *87*, 5357–5361.
[24] a) K. Palmo, J.-O. Pietila, B. Mannfors, A. Karonen, F. Stenman, *J. Mol. Spectrosc.* **1983**, *100*, 368–376; b) D. M. Chipman, M. F. Prebenda, *J. Phys. Chem.* **1986**, *90*, 5557–5560.
[25] G. N. R. Tripathi, *J. Am. Chem. Soc.* **1998**, *120*, 5134–5135.
[26] S. Fukuzumi, T. Okamoto, *J. Am. Chem. Soc.* **1994**, *116*, 11600–11601.
[27] In the case of **3**, the new absorption band, which appears at 570 nm, was overlapped with the absorption band at 590 nm due to the Cu^{I}–Q complex.
[28] S. Fukuzumi, M. Patz, T. Suenobu, Y. Kuwahara, S. Itoh, *J. Am. Chem. Soc.* **1999**, *121*, 1605–1606.
[29] a) S. Fukuzumi, T. Suenobu, M. Patz, T. Hirasaka, S. Itoh, M. Fujitsuka, O. Ito, *J. Am. Chem. Soc.* **1998**, *120*, 8060–8068; b) M. Patz, Y. Kuwahara, T. Suenobu, S. Fukuzumi, *Chem. Lett.* **1997**, 567–568.
[30] R. N. Bagchi, A. M. Bond, F. Scholz, R. Stösser, *J. Am. Chem. Soc.* **1989**, *111*, 8270–8271.
[31] A similar ESR spectrum has been reported for $O_2^{\bullet-}$ adsorbed on ZnO; A. J. Tench, T. Lawson, *Chem. Phys. Lett.* **1971**, *8*, 177–178. In this case, the equivalent ^{17}O hyperfine interaction indicates the side-on coordination of $O_2^{\bullet-}$ to the Zn^{II} ion. In the case of the $O_2^{\bullet-}$ complexes with **5** and **6**, the type of coordination has yet to be determined.
[32] a) W. Känzig, M. H. Cohen, *Phys. Rev. Lett.* **1959**, *3*, 509–510; b) H. R. Zeller, W. Känzig, *Helv. Phys. Acta* **1967**, *40*, 845–872.
[33] P. H. Kasai, *J. Chem. Phys.* **1965**, *43*, 3322–3327.
[34] The spin-orbit coupling constant λ is the function with regard to each atom, which decreases rapidly to zero with increasing distance from the atomic nucleus. Thus, the *l* value of oxygen atom can be used in Equation (2), see: A. Carrington, A. D. McLachlan, *Introduction to Magnetic Resonance with Applications to Chemistry and Chemical Physics*, Harper & Row, New York, **1967**.
[35] The $g_{\|}$ values of $O_2^{\bullet-}$ adsorbed on ZnO (2.042–2.052) are also significantly smaller than the values on MgO (2.077); this indicates that the Lewis acidity of the Zn^{II} ion is stronger than that of the Mg^{II} ion; see: J. H. Lunsford, *Catal. Rev.* **1973**, *8*, 135–157.
[36] D. D. Perrin, W. L. F. Armarego in "*Purification of Laboratory Chemicals*", Butterworth–Heinemann, Oxford, **1988**.
[37] K. Wallenfels, M. Gellerich, *Chem. Ber.* **1959**, *92*, 1406–1415.
[38] S. Fukuzumi, T. Yorisue, *Bull. Chem. Soc. Jpn.* **1992**, *65*, 715–719.

Received: May 2, 2001 [F3232]